Multifunctional Hydrogels

13

Min Xu and Hailong Huang

Contents

Abstract

Hydrogels are cross-linked three-dimensional polymeric networks which can absorb a great quantity of water and keep mechanically stable without dissolution. Due to the biocompatibility and biodegradability, biological hydrogels have been

M. Xu (✉) · H. Huang

School of Physics and Materials Science and Shanghai Key Laboratory of Magnetic Resonance, East China Normal University, Shanghai, China

e-mail: mxu1@uakron.edu; xumin@phy.ecnu.edu.cn; huanghao3310774@163.com

wildly investigated and used in various fields, such as adsorption materials, shape memory materials, self-healing materials, sensor units, super capacitor, drug carriers, and so on. In this chapter, we would focus on some of the upper aspects and give a brief introduction.

1   Introduction

Hydrogels are three-dimensional hydrophilic polymeric networks and are typically soft and elastic, owing to their compatibility with water. Cross-links and interconnections, which make polymer chains get together, can be formed by physical entanglements or chemical bonds, leading to physical and chemical hydrogels. Chemical hydrogels can be formed by chemical reactions such as radical polymerization [1], photopolymerization [2], high-energy radiation [3], and covalent conjugation [4]. These hydrogels generally show good physical stability and mechanical strength. Physical hydrogels are composed of polymer self-aggregation via non-covalent interactions such as hydrogen bonds [5], hydrophobic interactions [6], electrostatic interactions [7], inclusion complex [8], π–π stack [9], ionic interactions [10], crystallinity [11], and other affinity interactions [12]. These hydrogels exhibit excellent swelling and absorption capacities. Based on the raw materials and synthetic methods, the hydrogels can be classified to be petroleum-based hydrogels or bio-based hydrogels, covalent or physical hydrogels, copolymer networks or interpenetrating networks, degradable or nondegradable hydrogels, and so on. Due to their unique characteristics, hydrogels have been extensively studied in bioscience and material science and widely applied as functional materials, for example, contact lenses [13], disposable diapers [14], wastewater treatments [15], and moist pads for healing wounds [16] or burns [17]. In this chapter, we would like to introduce the advanced research and applications as follows: (1) adsorption hydrogels, (2) stimuli-responsive hydrogels, and (3) self-healing hydrogels.

2   Adsorption Hydrogels

Attributed to the network structure, hydrogels have excellent adsorption capacity to absorb large quantity of water and keep stability. Through designing functional molecular or modifying natural products, the hydrogels can provide complexing sites for the templates as adsorption materials. Recently, lots of researches are dealing with the use of hydrogels for adsorption materials, and also many researchers are investigating the hydrogels for wastewater treatments.

2.1   Wastewater Treatments

With the development of industry, environmental pollution has received great attention and became the focus of research. Water pollution, especially heavy metal ions and organic dye, is a menace to health. Many methods are used to purify water, such as chemical separation, electrochemical separation, adsorption, and cation exchange. Among these methods, adsorption is the most high-efficient method with high adsorption capacity, selectivity, and reusability. In recent years, many researchers pay attention to natural materials and polymer composites for the removal of pollutants from water, which have received excellent achievements.

2.1.1   Broad Adsorption of Heavy Metal Ions

Biomaterials, such as cellulose, chitosan, and their composites, are fitful to be the matrix to prepare adsorption materials for heavy ions [18–22]. A typical composite is cellulose–polyetherimide (PEI) composite hydrogel [23]. It was prepared in alkali/urea solution system with PEI as functional group and cellulose as skeleton in Fig. 1. The composite hydrogel showed good adsorption capacity of heavy metal ions such as Cu(II) 253.8 mg/g, Ni(II) 112.2 mg/g, Zn(II) 148.4 mg/g, Cr(III) 30.4 mg/g, and Pb(II) 248.2 mg/g as shown in Fig. 2. The thermodynamics and kinetics of the system were also studied. The adsorption process followed pseudo-second-order kinetics equation, and the adsorption capacities of cellulose/PEI composite hydrogel were much higher than activated carbon-based adsorption materials. Hence, cellulose/PEI composites could be potential materials for wastewater treatments and the recycling applications of heavy metal ions.
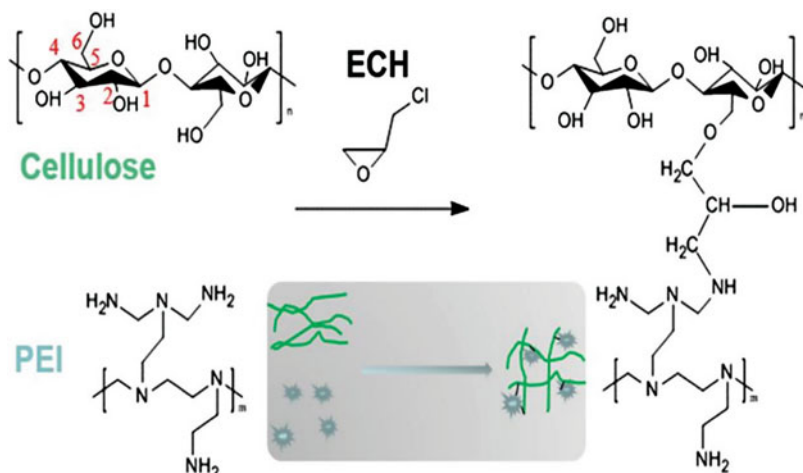

Fig. 1 Proposed mechanism for cross-linking reaction of cellulose and PEI in alkali aqueous solution with epichlorohydrin (ECH)

Fig. 2 (a) Effect of contact time on adsorption of cellulose/PEI composites. Conditions: initial concentration, 500 mg/L; room temperature. CP-1, cellulose/PEI (4:5, wt%); CP-2, cellulose/PEI (2:5, wt%); CP-3, cellulose/PEI (2:10, wt%); CP-4, cellulose/PEI (2:20, wt%). (b) The adsorption capacity of cellulose/PEI composite on Zn(II), Ni(II), Cr(III), Pb(II), and Cu(II). Conditions: cellulose/PEI composite (CP-2); initial concentration, 1000 mg/L; adsorption contact time, 80 h; room temperature
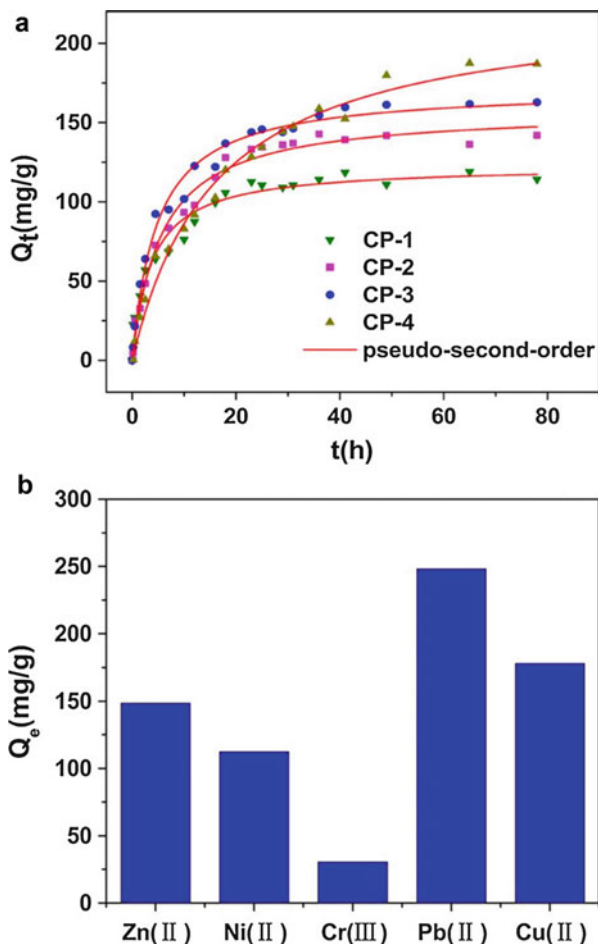
Because of efficient separation, magnetic technology has become an attractive method to solve the recycling problems of adsorption material. In recent studies, carboxylated cellulose nanofibrils(CCNFs)-filled magnetic chitosan hydrogel beads [24] (m-chitosan/poly(vinyl alcohol)/CCNFs) were prepared by an instantaneous gelation method as shown in Fig. 3. The magnetic hydrogel was used as adsorbents for Pb(II) ions (171.0 mg/g). The adsorption isotherm was fitted by the Langmuir model and the adsorption kinetics closed to pseudo-second-order model. Moreover, the hydrogel could be easily separated by magnetic field and regenerates in weak acid solution. It showed good reusable ability after four cycles keeping 90% adsorption capacity. M-chitosan/poly(vinyl alcohol)/CCNFs hydrogel could be considered as a promising adsorbent for the removal of Pb(II) ions for the high adsorption capacity, fine biodegradability, and the ability to be rapidly separated from aqueous solution (Fig. 4).
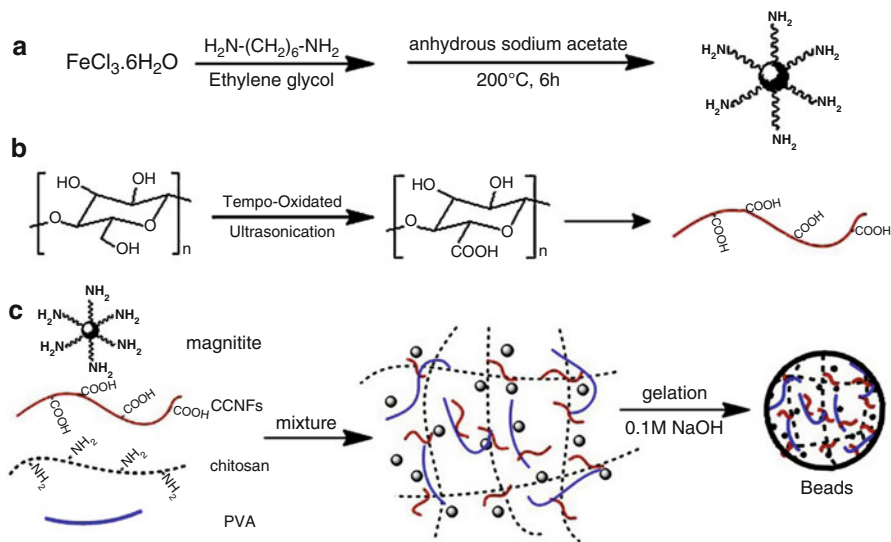
Fig. 3 Proposed mechanistic pathway for the preparation of magnetite nanoparticles (**a**), CCNFs (**b**), and m-CS/PVA/CCNFs hydrogels (**c**)

2.1.2 Selective Adsorption of Metal Ions

Sometimes, we need to recycle some certain metal ions, for example, lithium ion. Due to the large solubility product constant of lithium carbonate, the lithium ion is very difficult to be completely retrieved. Many methods have been developed to retrieve lithium ion, such as biological recovery, precipitation recovery, and adsorption recovery. Among them, adsorption is a cost-effective and environmental friendly method for recovering lithium from aqueous solution. However, most adsorbents are nonspecific, showing low selectivity toward a specific metal. Therefore, a novel magnetic ion-imprinted polymer (IIP) with a core–shell structure ($Fe_3O_4@SiO_2@IIP$) [25] was synthesized by a surface imprinting technique using 2-(allyloxy)methyl-12-crown-4 as the functional monomer, lithium ion as the template, and ethylene glycol dimethacrylate as the cross-linker (as shown in Fig. 5). $Fe_3O_4@SiO_2@IIP$ showed fast adsorption kinetics for lithium ion (10 min to reach complete equilibrium), and the adsorption process obeyed an external mass transfer model. Homogeneous binding sites were proved by the Langmuir isotherm, and the maximum adsorption capacity was 0.586 mmol/g. $Fe_3O_4@SiO_2@IIP$ showed excellent selectivity for Li(I), and the selectivity separation factors of Li(I) with respect to Na(I), K(I), Cu(II), and Zn(II) were 50.88, 42.38, 22.5, and 22.2, respectively, as shown in Fig. 6. The adsorption capacity of the adsorbent remained above 92% after five cycles. This study offered a good method for Li's recovery.

2.1.3 Adsorption of Organic Dyes

A novel environmental friendly composited hydrogels of hydroxypropyl cellulose (HPC) and molybdenum disulfide (MoS_2) were prepared [26]. The obtained
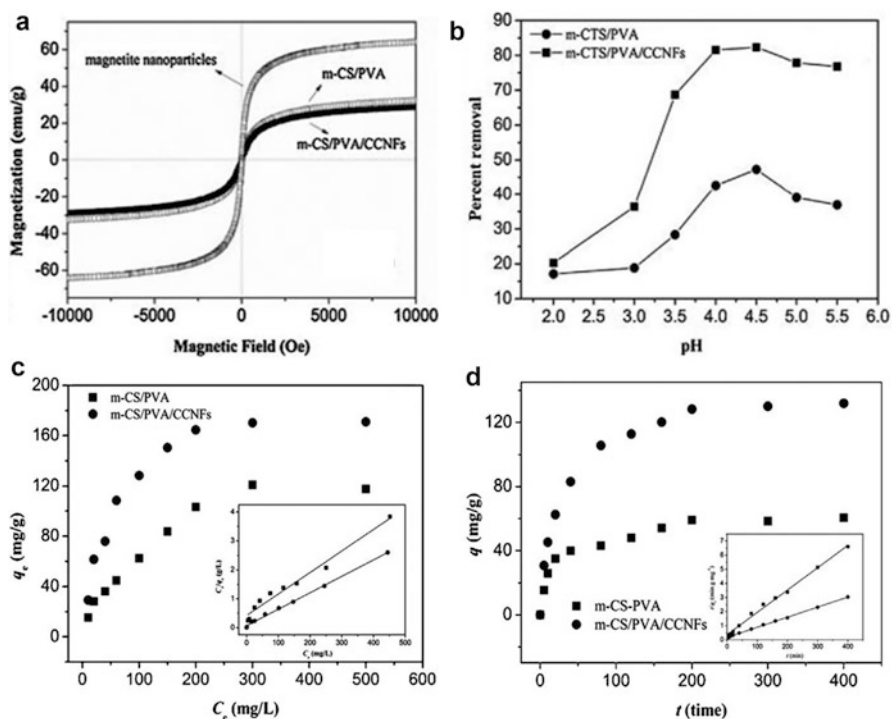
Fig. 4 (**a**) Magnetization curves of magnetite nanoparticles and hydrogels at room temperature. (**b**) Effect of pH on the Pb(II) ion uptake by m-CS/PVA and m-CS/PVA/CCNFs hydrogels. Adsorption isotherms (**c**) and adsorption kinetics (**d**) of Pb(II) ion uptake on m-CS/PVA and m-CS/PVA/CCNFs hydrogels. The inset shows the fitting results by the Langmuir isothermal model (**c**) and pseudo-second-order model (**d**)

HPC-M_oS_2/HPC hydrogels showed an enhanced adsorption behavior for methylene blue (Fig. 7a). The adsorption kinetics and isotherms were studied with different models. It indicated that the adsorption system followed predominantly the second-order rate model, and the adsorption process was mainly monolayer and took place on a homogeneous surface. More important, it could be reused to catalyze the degradation of methylene blue upon exposure to the sunlight as shown in Fig. 7b. The absorbed dyes in MoS_2-HPC/HPC hydrogels could be degraded upon exposure to sunlight, and then the hydrogels were circularly used to absorb dyes again. Considering the recycling properties of low-cost and biocompatible cellulose, the composite hydrogels will become promising candidates to remove dyes from effluents.

2.2 Drug-Selective Adsorption, Delivery, and Release

Hydrogels are hydrophilic polymer networks that can absorb more than 100 times their dry weight in water, giving the physical characteristics like soft tissue. In

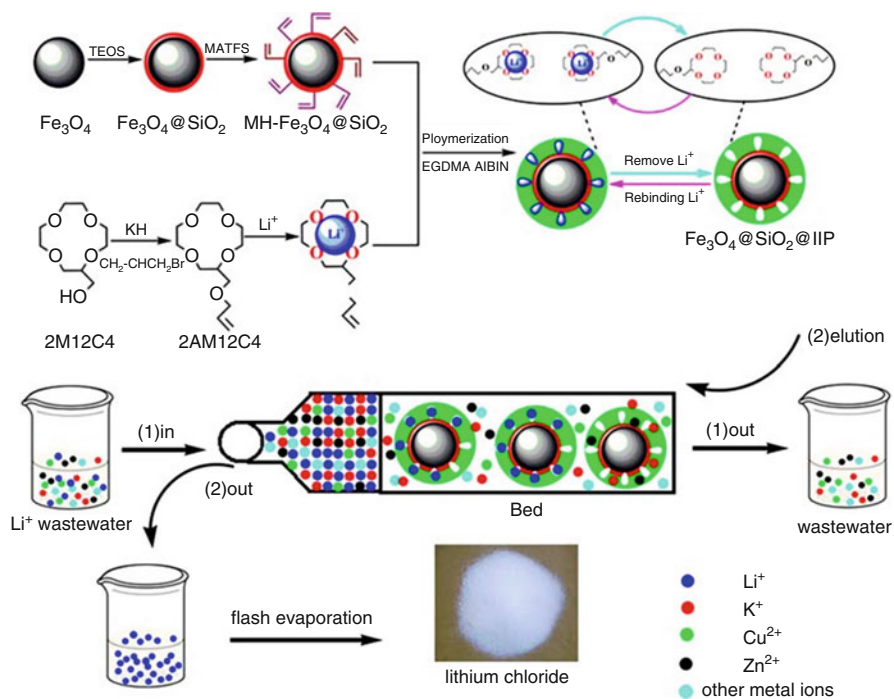**Fig. 5** Synthesis route for $Fe_3O_4@SiO_2@$ion-imprinted polymer

Fig. 6 Selective adsorption of Li(I) by $Fe_3O_4@SiO_2@IIP$ and $Fe_3O_4@SiO_2@NIP$. Conditions: 50 mg of adsorbent, 50 mL of Li(I) with 10 mmol/L, and temperature of 25 °C
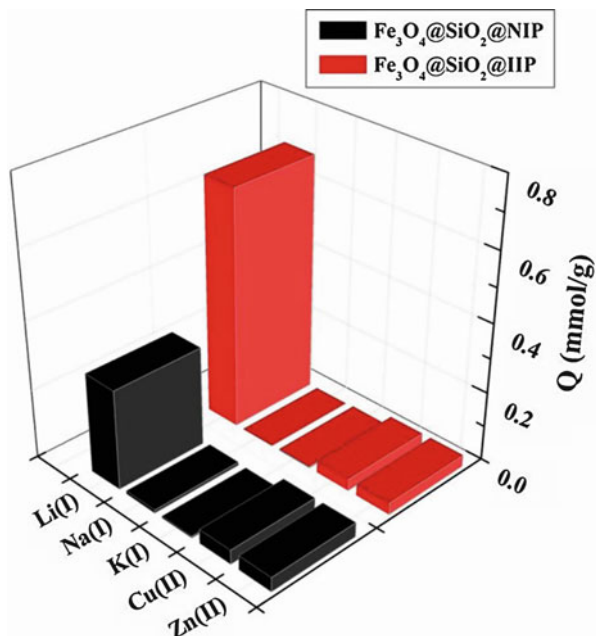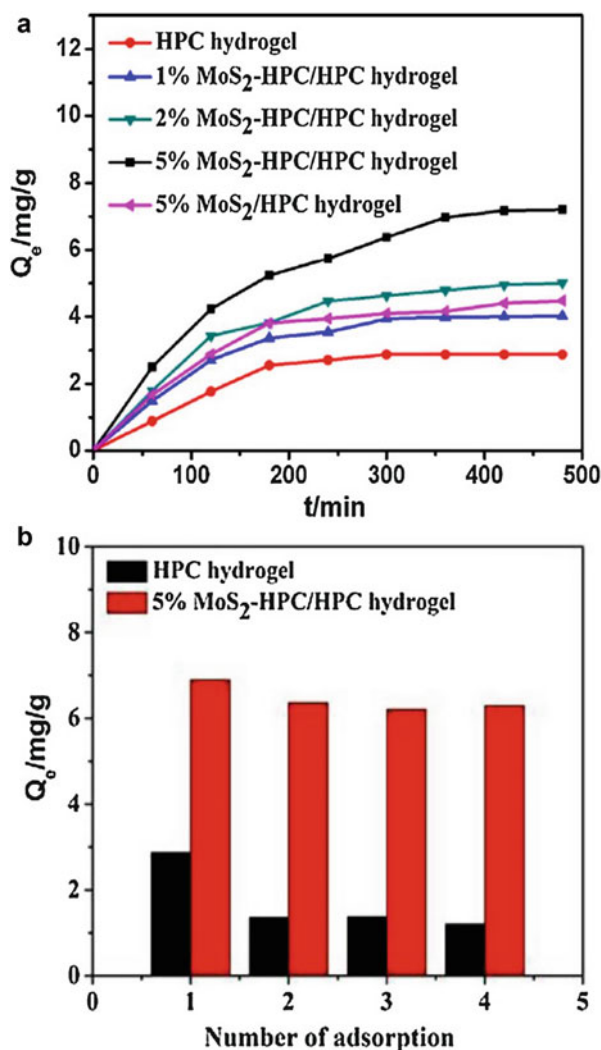
Fig. 7 (**a**) Time profile of methylene blue removal on hydrogel. The hydrogel was 0.19 g and the initial concentration of methylene blue was 50 ppm. (**b**) The photo-induced recycling properties of HPC hydrogel and 5% MoS2-HPC/HPC hydrogel

addition, hydrogels are highly permeable which facilitate exchanges of oxygen, nutrient, and other water-soluble metabolites. Thus, hydrogels are being investigated as drug delivery system due to their potential which can control the transport and release of macromolecular drugs such as pesticides [27–29], proteins [30–32], and nucleotides [33]. The diffusion mechanism of solute molecules within hydrogels is of great interest for a wide variety of industrial applications.

Recently, functional hydrogels are wildly studied in many fields, especially in drug delivery [34–36] and release aspects [37–39]. Molecularly imprinted magnetic cellulose microspheres (MIP-MCM) [40] were developed by a surface functional monomer-directing system. A layer of MIP was coated on the surface of the
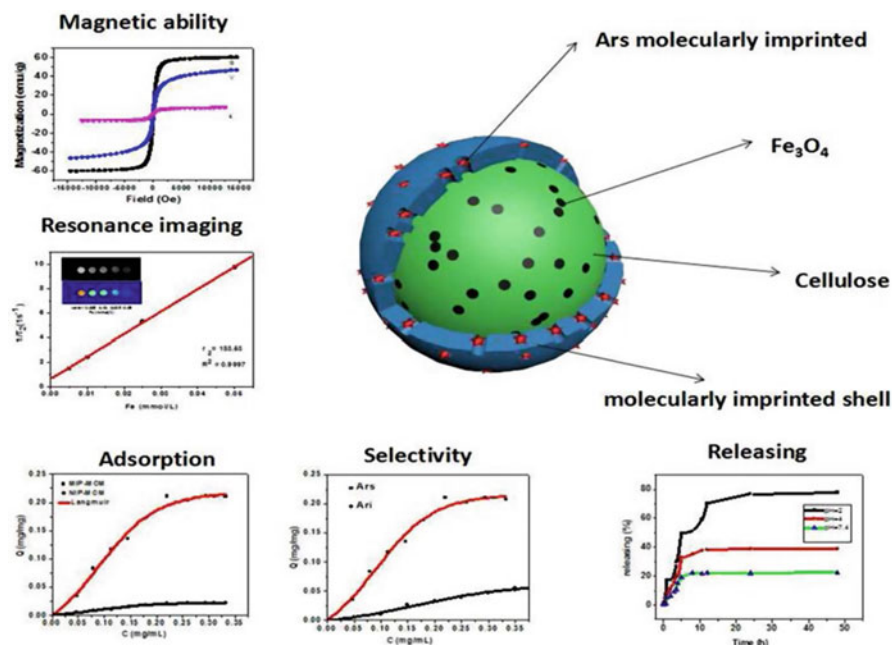
Fig. 8 Schematic procedure for molecularly imprinted magnetic cellulose microsphere preparation

cellulose microspheres in which Fe_3O_4 nanoparticles were embedded before. The process of preparation was shown in Fig. 8. By selecting artesunate (Ars) as template, the product showed high selectivity to Ars. Meanwhile, the MIP-MCM also showed highly regenerate and stable in wide pH and temperature ranges. The adsorption of Ars reached equilibrium within 10 h, and the maximum adsorption quantity was as high as 0.22 mg/mg. Through the Langmuir–Freundlich isotherm and pseudo-second-order kinetic model, the thermodynamic studies suggested that the adsorption of Ars on MIP-MCM was a spontaneous process. MIP-MCM also showed rapid magnetic separation and high reusability (retained 90% adsorption quantity after five cycles). Furthermore, MIP-MCM was good negative MRI contrast agents with good biocompatibility. Due to these properties, this work offered a new potential application for MIP-MCM in aspects of drug delivery, tracking, disease diagnosis, and therapy.

P(2-hydroxyethylmethacrylate/methacralic acid) hydrogels [41] were synthesized by gamma radiation-induced copolymerization of 2-hydroxyethylmethacrylate (HEMA) and methacrylic acid (MAA) in aqueous solution. The hydrogels as carrier for the drug adsorption and controlled release capacities of chlortetracycline HCl were investigated (see Fig. 9). The adsorption and release processes were stable in wide pH and temperature ranges. The influence of MAA content of hydrogels on the adsorption capacities was studied. The adsorption capacity of chlortetracycline HCl increased from 8 to 138 mg per gram dry gel with increasing amount of MAA in the gel system. The release of chlortetracycline HCl from the poly (HEMA/MAA)
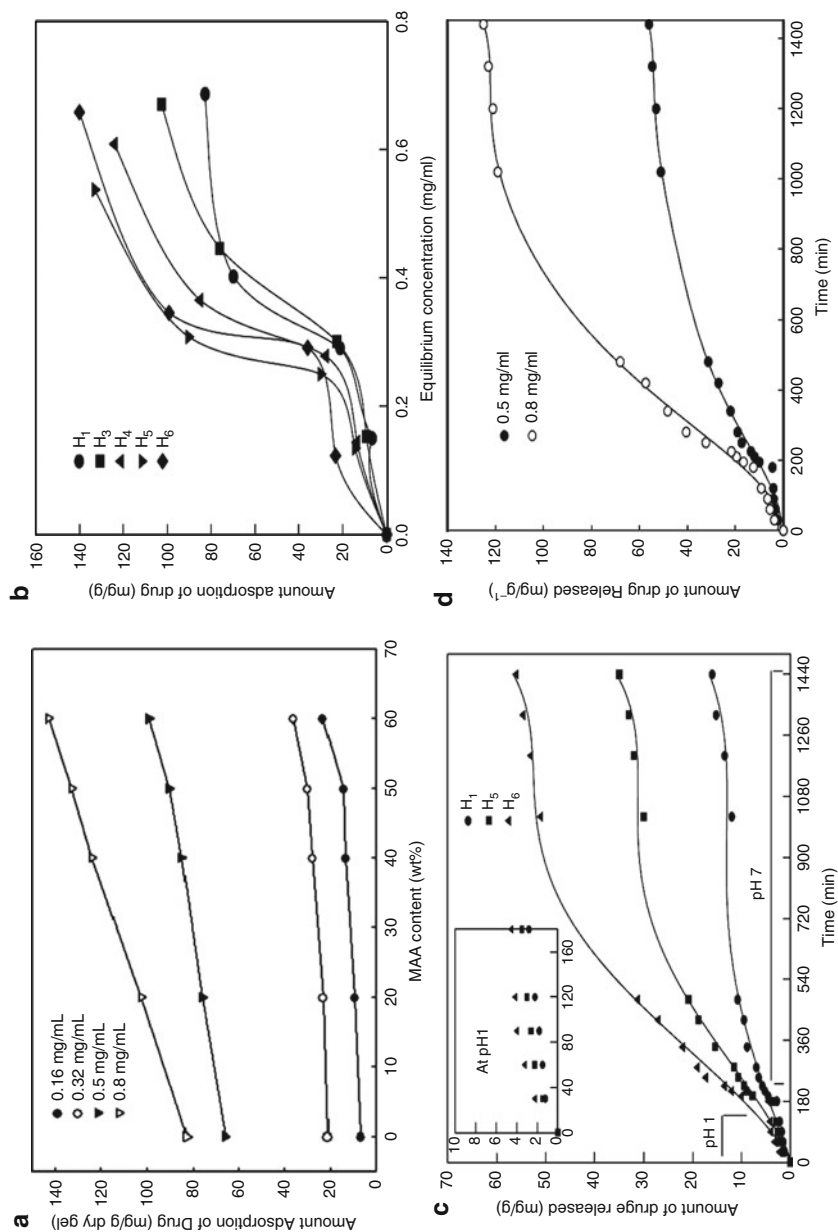
Fig. 9 (**a**) Effect of MAA content on the amount adsorption (mg/g) of (HEMA/MAA) hydrogels, at different drug concentrations. (**b**) Relationship between equilibrium concentration of chlortetracycline HCl and its amount adsorption (mg/g) for different (HEMA/MAA) compositions. (**c**) Chlortetracycline HCl

hydrogels, as studied at the physiological temperature of 37 °C, exhibited a strong pH-dependent release behavior, which offers minimum release at pH 1.0 and maximum release at pH 7–8.

3   Stimuli-Responsive Hydrogels

Stimuli-responsive hydrogels are a broad class of hydrogels whose swelling or deswelling processes, gel-to-solution or gel-to-solid transitions, and shapes can respond to the physical or chemical external stimuli, such as temperature, pH, magnetic, ultrasonic, electrochemistry, or light. Different kinds of stimuli-responsive hydrogels are used in various areas, like sensors [42, 43] and actuators, display and image devices [44–46], conditional controlled drug delivery [27–33], and so on. There are many different synthetic methods and sources to prepare stimuli-responsive hydrogels and exploit different applications.

3.1   pH- and Temperature-Sensitive Hydrogels

Temperature- and pH-sensitive hydrogels are most wildly investigated. Recently, some dual- even multi-stimuli-responsive hydrogels are developed. A novel poly((2-dimethylamino) ethyl methacrylate) PDMAEMA and poly ((2-dimethylamino) ethyl methacrylate-*co*-butyl methacrylate) P(DMAEMA-co-BMA) hydrogels were studied on the mechanical properties and pH- and temperature-sensitive swelling behaviors [47]. Mechanical measurements showed that the addition of hydrophobic comonomer butyl methacrylate (BMA) increased the mechanical strength of the network. Swelling studies showed that these hydrogels were both pH- and temperature-sensitive (see Figs. 10 and 11). It was possible to control the pH- or temperature-sensitive phase transition characteristics of these hydrogels without changing the chemical structure by a change in temperature or pH of the surrounding environments, respectively. Additionally, it also likely to further tailor the phase transition properties of the hydrogels by incorporation of a hydrophobic comonomer butyl methacrylate (BMA). Increasing the BMA content of the hydrogel chemical structure reduced the phase transition points of the temperature and pH.

Fig. 9 (continued) released from different (HEMA/MAA) compositions as a function of time, at two pH values (pH 1 at time up to 180 min and pH 7 at time above 180 min) and at constant concentration of drug 0.5 mg/ml. (**d**) Chlortetracycline HCl released from (HEMA/MAA) (40/60) hydrogels as a function of time for different loaded amounts of drug, at two pH values (pH 1 at time up to 180 min and pH 7 at time above 180 min)
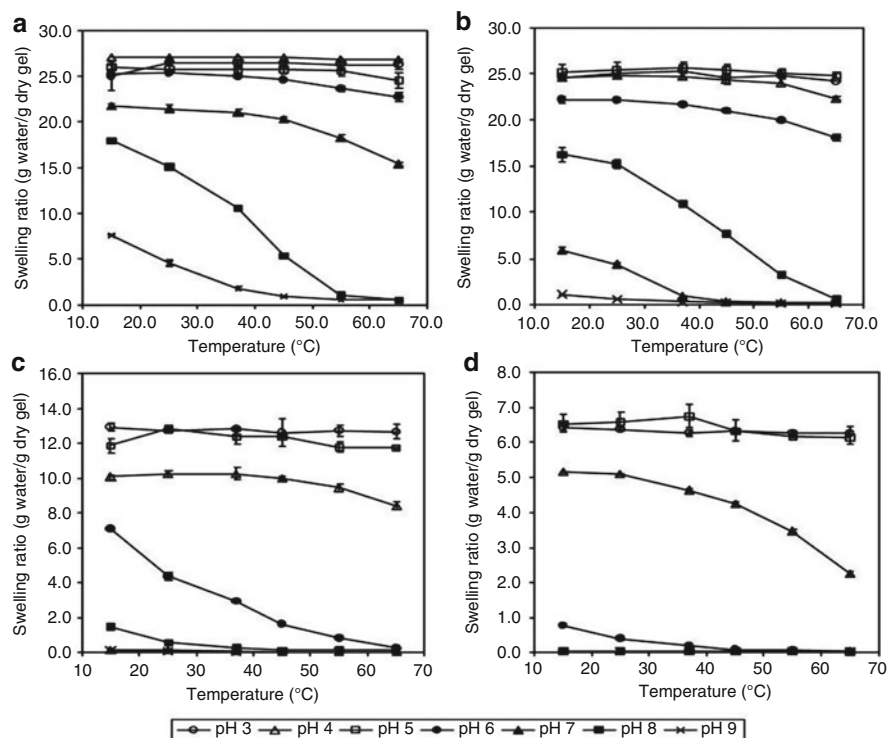
Fig. 10 Swelling ratio of the poly((2-dimethylamino) ethyl methacrylate-*co*-butyl methacrylate) hydrogels as a function of temperature at different values of pH. (**a**) 0% butyl methacrylate; (**b**) 20% butyl methacrylate; (**c**) 40% butyl methacrylate; (**d**) 60% butyl methacrylate

3.2 Light-Sensitive Hydrogels

Due to their remotely triggerable releasing ability and combinational functionalities, light-responsive hydrogel particles are applied in microreactor, drug delivery, and tissue engineering. Light stimuli can be used for remote and noninvasive switching of the therapeutic agents' flux. Near-infrared (NIR) light can penetrate body tissue with limited absorbance. Thus, NIR light-responsive hydrogel particles with desirable compartmental structures were produced using suspended agarose/alginate pre-gel droplets induced by a superhydrophobic surface as templates [48] as shown in Fig. 12. The agarose/alginate double-network hydrogel was synthesized via a two-step sequential gelation process. The synthesized hydrogel particles, when loaded with polypyrrole (PPy) nanoparticles that act as photothermal nano-transducers, were demonstrated to function as near-infrared (NIR) light triggerable and deformation-free hydrogel materials. Compared with the massive release of tetramethyl rhodamine isothiocyanate (TRITC)-dextran (≈45%) from the single-compartment particles induced by laser irradiation for 10 min, the release process was controlled and regulated to deliver 25% of the TRITC-dextran from the core-
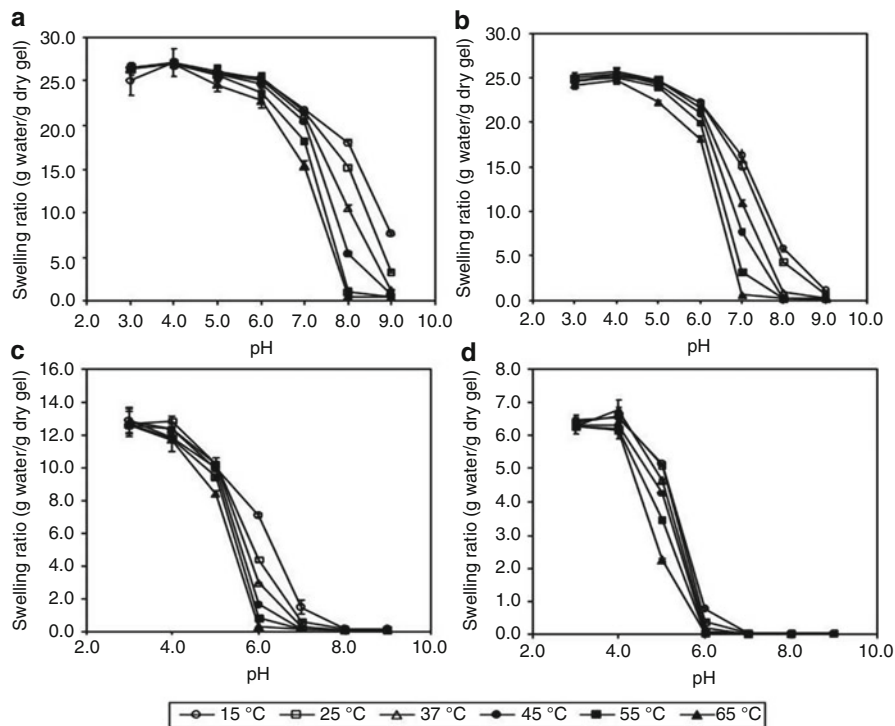
Fig. 11 Swelling ratio of the poly((2-dimethylamino) ethyl methacrylate-*co*-butyl methacrylate) hydrogels as a function of pH at different temperatures. (**a**) 0% butyl methacrylate; (**b**) 20% butyl methacrylate; (**c**) 40% butyl methacrylate; (**d**) 60% butyl methacrylate

shell structured particles. These multi-compartmental hydrogel particles exhibited tailored properties such as tunable particle size, tunable layer thickness, tunable layer number, and selective light sensitivity, which provided a wide range of options for drug encapsulation and remotely controlled release.

3.3   Electric-Sensitive Hydrogels

In recent years, capacitors have been extensively explored as an electrochemical device. The electrode materials are usually coated on the surfaces of current-collecting electrodes. The traditional current-collecting electrodes such as platinum, gold, or titanium are very expensive. The double-layer charges in thick electrode materials cannot be conveniently transferred to current-collecting electrodes (CCEs) and decrease the rate capability of electrochemical capacitors (ECs) with thick electrodes. A graphene hydrogel/nickel foam (G-Gel/NF) composite electrode was prepared by depositing reduced graphene oxide in the micropores of
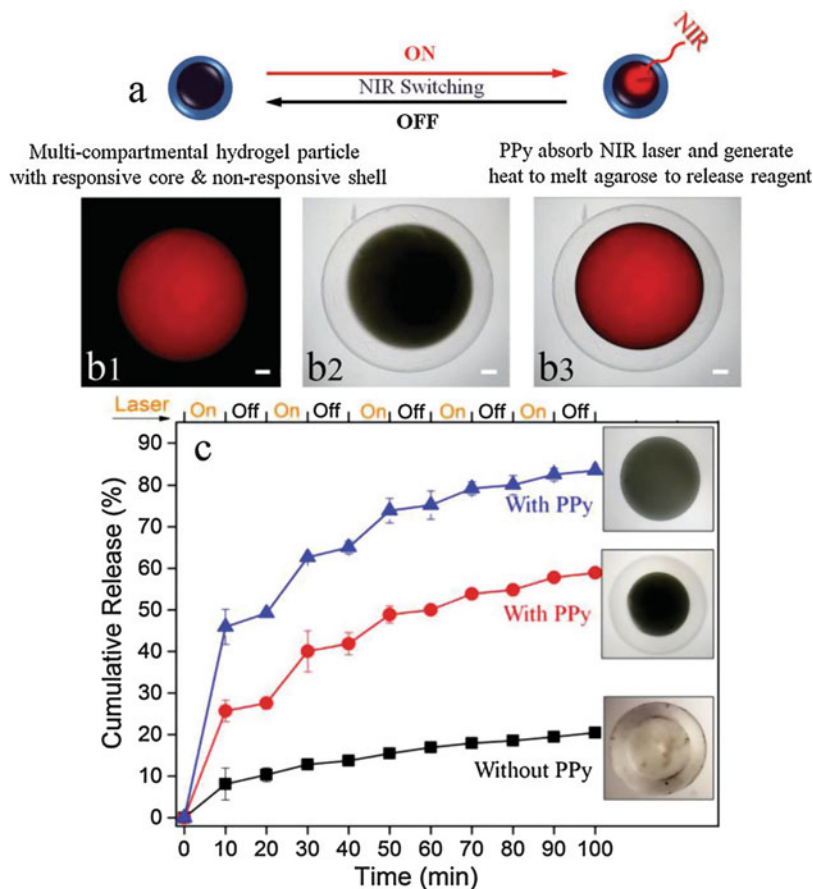
Fig. 12 (**a**) Schematic illustrations showing NIR laser-induced TRITC-dextran released from the multi-compartmental hydrogel particles with a core-shell structure, in which the PPy nanoparticles and the TRITC-dextran-loaded core exhibited NIR laser sensitivity, whereas the non-loaded shell was not responsive to NIR stimulation. (**b1**–**b3**) Microscope observation showing the multi-compartmental hydrogel particles with a core-shell structure, in which (**b1**) was a fluorescent microscope picture indicating the loading of TRITC-dextran in the hydrogel core, (**b2**) was a bright-field microscope picture indicating the loading of PPy nanoparticles in the hydrogel core, and (**b3**) was the overlay of (**b1, b2**) to indicate the multi-compartmental hydrogel particle with a loaded core and non-loaded shell. (**c**) NIR laser-induced release of TRITC-dextran from the hydrogel particles; the scale bar was 200 μm

nickel foam [49]. In this case, a thick (1.0 mm) G-Gel was separated into small pieces on the micrometer scale, and each of them was surrounded by Ni framework. Thus, the distances of ion/electron transportation in the electrodes were shortened. Consequently, the ECs based on thick G-Gel/NF electrodes (G-Gel/NF ECs) exhibited high specific capacitances (in terms of area), long durability, and high rate capability as shown in Fig. 13. Therefore, the G-Gel/NF electrodes not only
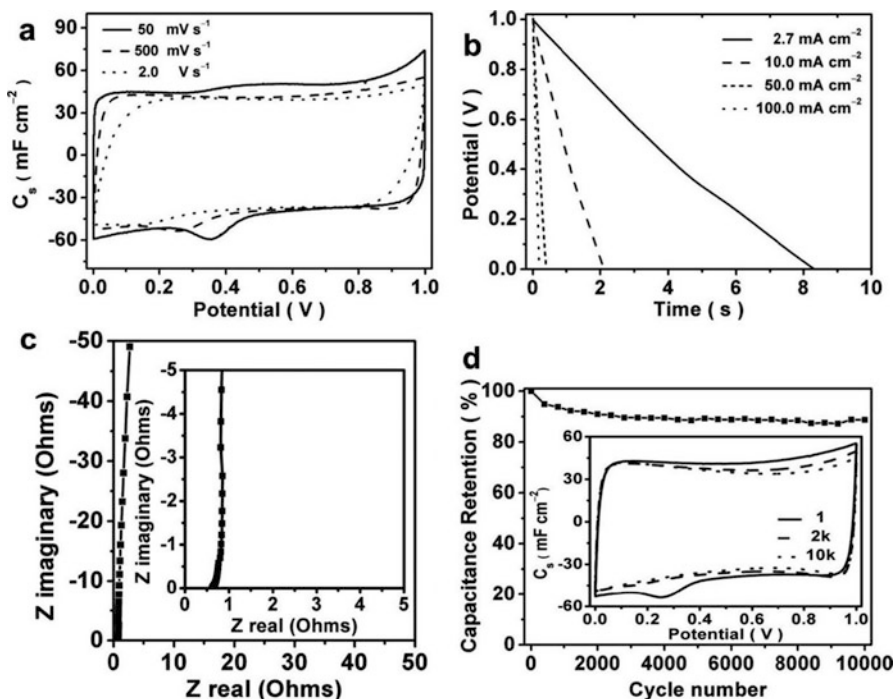
Fig. 13 (**a**) CV curves of G-Gel/NF EC in 5 M KOH at different scan rates. (**b**) Discharge curves of G-Gel/NF EC at different current densities. (**c**) Nyquist plot of G-Gel/NF EC. Inset: Plot on an enlarged scale. (**d**) Cycling stability of G-Gel/NF EC upon charging/discharging at a current density of 10 mA cm^{-2}. Inset: CV curves recorded before and after charging/discharging for 2000 or 10,000 cycles; scan rate = 500 mV s^{-1}

exhibited large specific capacitance and long cycling life but also showed high rate performance. By this way, the graphene material and current-collecting electrode were built in one piece without occupying additional volume. Furthermore, the micropores of G-Gel were exposed to the electrolyte for the access of ions to form electrochemical double layers, and the nickel framework shortened the distances of charge transfer.

An interpenetrating polymer networks (IPNs) composed of hyaluronic acid (HA) and poly(vinyl alcohol) (PVA) hydrogels [50] were prepared, and the effects of various pH conditions and electric field on swelling ability were investigated. The IPN hydrogels exhibited pH-sensitive and electro-responsive properties (see Fig. 14). The IPN hydrogels exhibited a relatively high swelling ratio as HA content is increasing. The HA–PVA (3:1, wt%) sample containing the highest HA content among samples showed the highest swelling ratio of pH-dependent swelling behaviors. IPN hydrogels showed electro-responsiveness as shrinking and expanding reversibly with the on–off switching of the electric field. HA–PVA IPN hydrogel showed the greatest electro-responsiveness volume change with the composition of HA–PVA (1:1, wt%).

Fig. 14 (**a**) pH-dependent
swelling behavior of
HA–PVA IPN hydrogels. (**b**)
Electro-responsiveness of
HA–PVA IPN hydrogels due
to on–off switching of electric
field (5 V). HA–PVA (1:1,
wt%), HA–PVA (1:3, wt%),
HA–PVA (3:1, wt%)
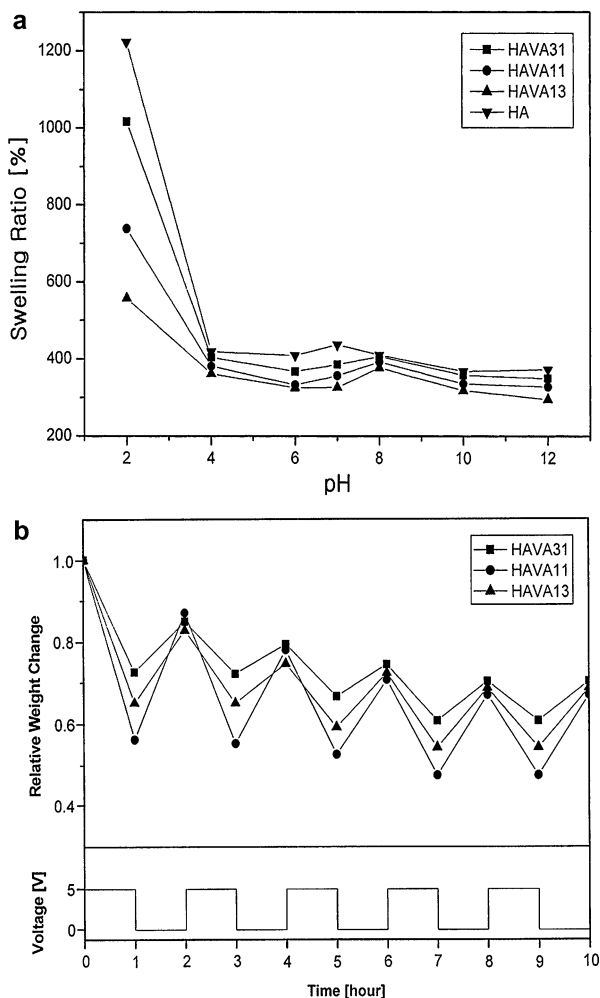
3.4   Dissolving Hydrogels

The controllable dissolving hydrogel is another trigger. By external stimuli, the
hydrogel can undergo gel-to-solution or reversible phase transitions. On-demand
dissolution biocompatible hydrogels [51] were synthesized by thiol−thioester
exchanging reactive groups as functional units for aqueous dissolution. When
hydrogels was stimulated in water, the thiol−thioester could hydrolyze. The rates
of exchange and hydrolysis depended on the temperature and pH of the solvent. The
dissolution of thiol−thioester hydrogels was shown in Fig. 15. These hydrogels
could be applied as wound dressings which would provide service as a protective
barrier against bacterial infection. The management and closure of wounds after
traumatic injury or surgical intervention are of significant clinical importance.
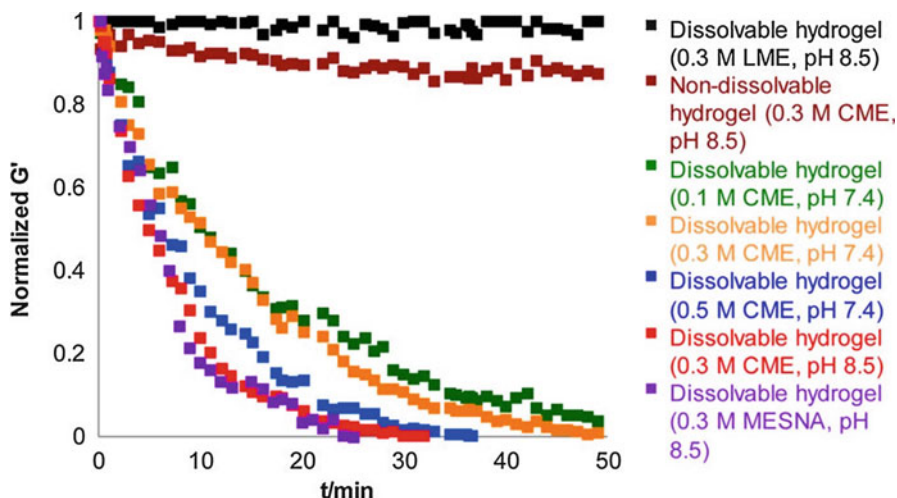
Fig. 15 Hydrogel dissolution as monitored by rheometry

Stimuli-responsive hydrogels that function as sealants, adhesives, or dressings are emerging as vital alternatives to current standards of care that rely upon conventional sutures, staples, or dressings.

3.5   Shape Memory Hydrogels

The "shape memory" effect is defined as an elastic deformation (programming) of a sample into a temporary shape stabilized by reversible covalent or physical cross-links. Shape memory hydrogels can form into a temporary shape and recover the original shape by external stimuli such as temperature, light, pH, or electricity. Based on the biocompatibility, the hydrogels have many biomedical or sensory applications, such as smart medical devices, implants for minimally invasive surgery, and heat-shrinkable tubing or films. The new shape memory hydrogels [52] sensitive to Fe^{3+}, pH, and temperature with tunable mechanical properties were presented in Fig. 16. Three programmable reversible systems including PBA-diol ester bonds (the reversible PBA-diol ester bonds formed by phenylboronic acid groups (PBA) and adjacent hydroxyl groups of glucosamine), AAc–Fe^{3+} (the coordination inter-actions between acrylic acid (AAc) and Fe^{3+} ions), and coil−helix transition of agar were applied to memorize temporary shapes and endowed the hydrogels with outstanding multishape memory functionalities.

3.6   DNA Hydrogels

Except normal materials, DNA, RNA, or nucleic acids also can be introduced into composite hydrogels as functional components. DNA can be precisely designed with
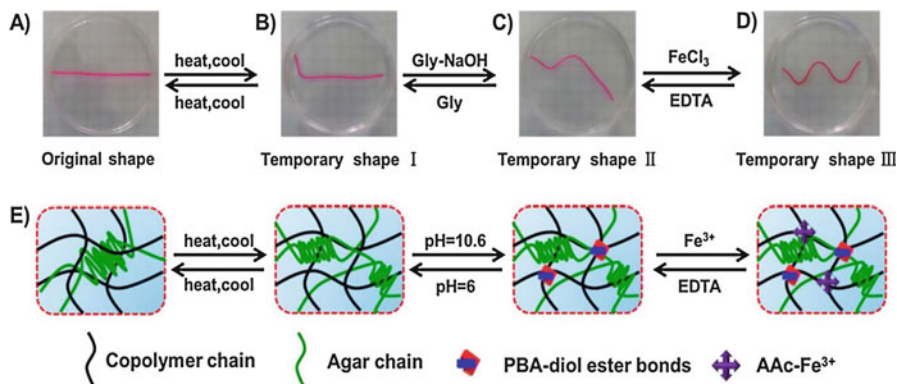
Fig. 16 Fe^{3+}, pH, and thermo-induced multishape memory effect. (**a, b**) Temporary shape I was fixed by coil–helix transition of agar upon changing the temperature. (**b, c**) Cross-links of dynamic PBA-diol ester bonds can be applied for memorizing temporary shape II. (**c, d**) Through the chelation between Fe^{3+} and carboxylic groups, temporary shape III can be fixed. (**e**) Mechanism of programmed multishape memory process

specific sequences and self-assemble into two- or three-dimensional structure to assemble nanoparticles. Through the cross-linked networks of DNA assembly, DNA hydrogels have great potential applications in biomaterials, such as drug and gene delivery, biosensing, and tissue engineering. In the past few years, many DNA hydrogels have been reported. The driving forces of the DNA hydrogels are physical interaction and chemical interaction. For physical interaction, DNA directly extracted from the nucleus in nature, like a long linear polymer, and formed a hydrogel via physical entanglement or by chemical cross-linking of small molecules. For chemical modification, DNA could be covalently grafted onto synthetic polymers and served as a cross-linker. The recognition of complementary DNA strands led to cross-linking of polymer chains and caused hydrogel formation.

A new and general platform created pure DNA hydrogels [53] through self-assembly as shown in Fig. 17. Two building blocks, a Y-scaffold and a linker, led to hydrogel formation. Moreover, by tailoring the DNA building blocks, the DNA hydrogels formed rapidly without any chemical treatment. The formation mechanism and properties of the DNA hydrogels were systematically studied. The DNA hydrogels reversibly responded to thermal stimulus, by switching between the gel and sol state across a transition temperature, as well as respond to enzymes when restriction sites are inserted into one of the building blocks. Therefore, it provided a new class of intelligent materials for a diverse range of biological and biomedical applications.

3.7 RNA Hydrogels

According to the self-assembled three-dimensional structures of oligonucleotides, it has showed promising applicability for imaging and gene delivery mainly using siRNAs. A novel RNA-triple-helix hydrogels [54] was prepared through programmable self-assembly of the two miR sequences to provide a stable and efficient nanovehicle for

Fig. 17 Schematic representation of DNA hydrogel formation. The Y-scaffold and linker are designed to cross-link by hybridization of their "sticky ends" (emphasized by green circles). By tailoring these "sticky ends" and inserting restriction sites in the linker sequences, the DNA hydrogels show thermal and enzymatic responsive properties
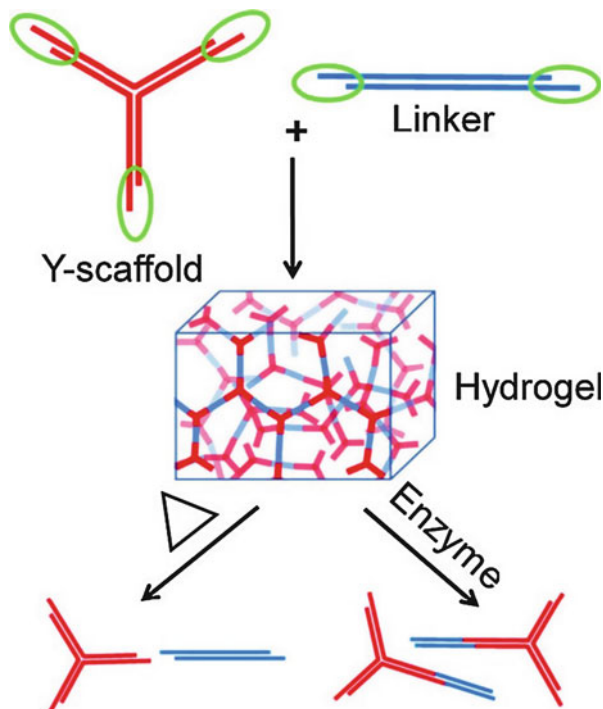
in vivo miR local delivery (see Fig. 18). Conjugating the RNA triple helix to dendrimer (triplex nanoparticles) formed an adhesive hydrogel upon mixing with dextran aldehyde controlled release of the two miRs. The RNA-triple-helix hydrogels was consisted of stable two-pair FRET donor/quencher RNA oligonucleotides.

Self-assembled RNA-triple-helix conjugates remained functional in vitro with high selective uptake and controlled over miRNA expression compared with their respective single-stranded or double-stranded forms (Fig. 19). This method provided a novel strategy for concomitant on miRNA inhibition and tumor suppressor miRNA replacement therapy using a RNA-triple-helix hydrogel scaffold that afforded highly efficacious local anticancer therapy. Hence, cancer gene delivery systems should provide potent, selective, and specific treatment to tumor cells only, unlike the standard delivery of most conventional chemotherapeutic drugs. This approach can be implemented to design self-assembled triplex structures from any other miR combination, or from other genetic materials, including antisense DNA or siRNA, to treat a range of diseases.

4 Self-Healing Hydrogels

Self-healing is one of the most remarkable properties of biological materials. The special ability of natural materials to heal cracks often involves an energy dissipation mechanism due to the so-called sacrificial bonds that break and reform dynamically
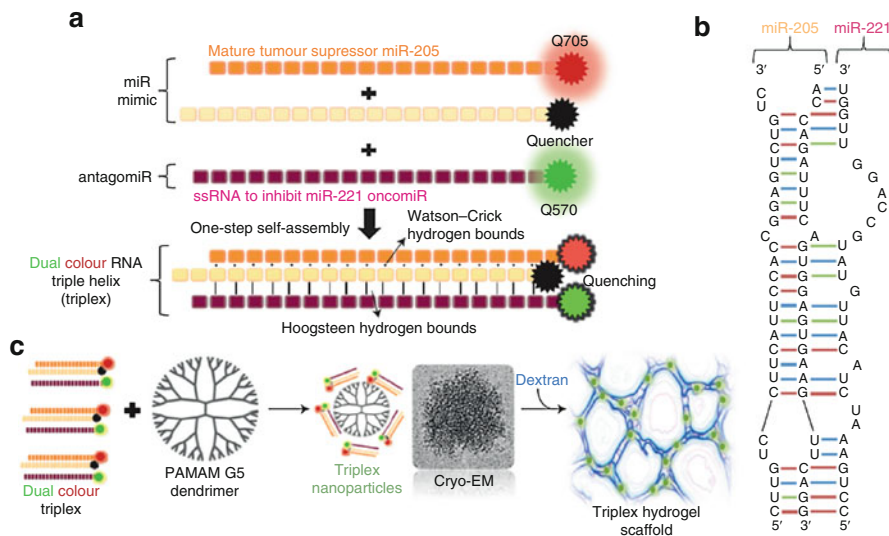
Fig. 18 Self-assembled RNA-triple-helix hydrogel nanoconjugates and scaffold for microRNA delivery. (**a**) Schematic showing the self-assembly process of three RNA strands to form a dual-color RNA triple helix. The RNA triplex nanoparticles consist of stable two-pair FRET donor/quencher RNA oligonucleotides used for in vivo miRNA inhibition (miR-221 antagomiR) strategy and miRNA replacement therapy (miR-205 mimic). (**b**) Secondary structure of an RNA triple helix bearing both miR-205 mimic and miR-221 antagomiR (structure produced/adapted using M-fold software). (**c**) Formation of the RNA-triple-helix hydrogel scaffolds by conjugation of the RNA-triple-helix structure to PAMAM G5 (Cryo-EM image showing the branched spongelike nanoscopic structure) followed by reaction with oxidized dextran to form the adhesive hydrogel

before the fracture of the molecular backbone. Numerous studies have been conducted in recent years to improve the mechanical performance of hydrogels. The self-healing materials which are capable of recovering their original mechanical performance after fracture require intermolecular non-covalent interactions. Although synthetic hydrogels are very similar to biological tissues, they are normally very brittle and lack the ability to self-heal, which hinders their use in any stress-bearing applications.

As new functional materials, self-healing hydrogels are under vast research nowadays for drug delivery, 3D cell proliferation, and tissue engineering. The broken self-healing hydrogels after damaged can regenerate the integral network and stay at the target position, enhancing the medicine delivery efficiency. This property can be introduced into macromolecules by the hydrogen bond driven through the creation of specific non-covalent intermolecular interactions. Moreover, self-healing systems can repair themselves autonomously, restoring the initial structures and functions without external stimulus after the interior or exterior cracks, which is similar to the ability of some living organisms (e.g., human skin). Constructing a non-covalently bonded system is an efficient approach to preparing self-healable polymeric hydrogels. Thus, introducing the self-healing feature to the
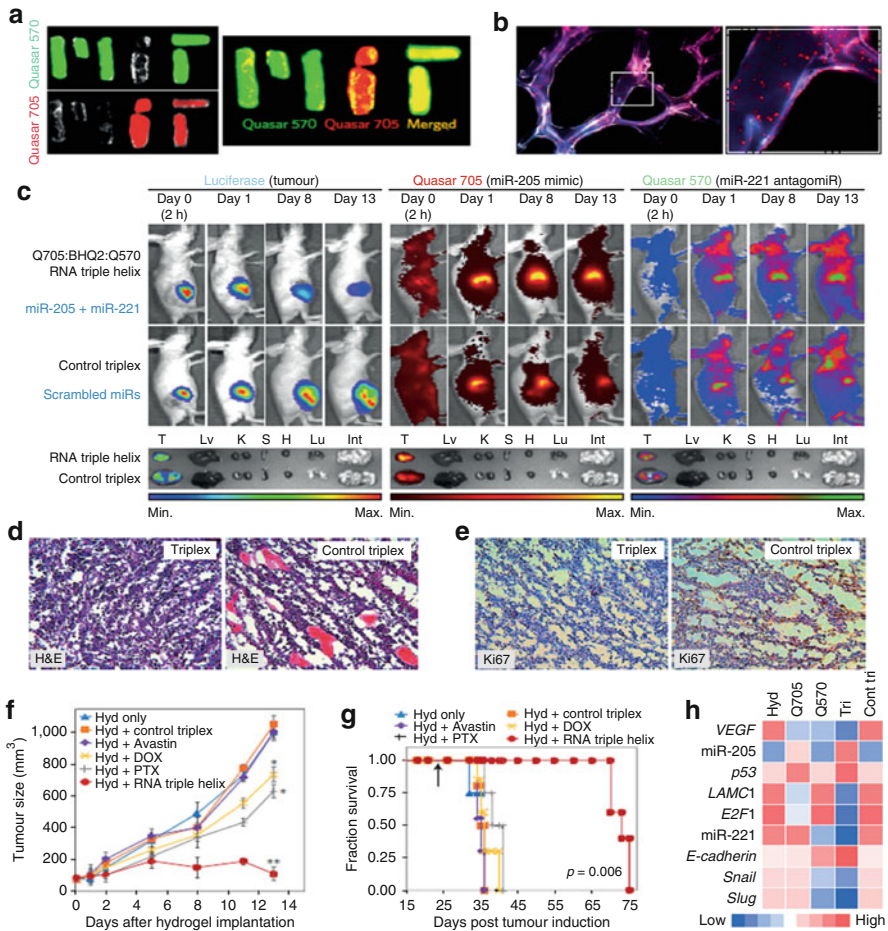
Fig. 19 In vivo miRNA modulation and tumor therapy via RNA-triple-helix hydrogel scaffolds. (**a**) Dual-color hydrogel scaffolds made of RNA-triple-helix nanoconjugates preincubated with complementary miR targets. (**b**) Cryosection of dendrimer–dextran adhesive hydrogel (12 μm thickness) depicting adhesive morphology (dextran aldehyde was tagged with Alexa Fluor 405). Red spots represent the triple-helix nanoparticles containing Q705 (red) and Q570 (green) oligonucleotides. (**c**) Live imaging of female SCID hairless congenic mice with triple-negative breast tumor xenograft implanted with hydrogels embedded with RNA-triple-helix nanoparticles and with a control triplex (scrambled miRs) (nD5 per group). Ex vivo images of breast tumors and whole body organs (T, tumor; Lv, liver; K, kidneys; S, spleen; H, heart; Lu, lung; Int, intestines) are also presented. (**d**) Hematoxylin and eosin (H&E) stains of tumors from treated groups with hydrogels embedded with RNA-triple-helix nanoparticles and with a control triplex (scrambled miRs). (**e**) Immunohistochemical evaluation of tumors treated with hydrogels embedded with RNA-triple-helix nanoparticles and with a control triplex for Ki67 to evaluate tumor cell proliferation. (**f**) Tumor size following treatment (nD5, statistical analysis performed with a two-way ANOVA, ∗∗, $P < 0.01$; ∗, $P < 0.05$). Individual tumors were measured using a Vernier caliper, and tumor volume was calculated by tumor volume (mm3) D width × (length2)/2. (**g**) Kaplan–Meier curves for mice treated with hydrogel scaffolds loaded with triple-helix and control triple-helix nanoparticles, as

hydrogel can improve the functionality and extend the application range of the hydrogel.

4.1   Self-Healing Hydrogels (Imine Bonds)

A straightforward method was used to prepare magnetic self-healing hydrogels by facilely mixing carboxyl-modified Fe_3O_4 nanoparticles in the self-healing hydrogels [55]. Due to the interaction between -NH_2 on chitosan and carboxyl groups on the Fe_3O_4 surface, the Fe_3O_4 nanoparticles could be dispersed well in chitosan solution to form a stable ferrofluid. This chitosan–Fe_3O_4 ferrofluid was subsequently mixed with difunctional poly(ethylene glycol) DF-PEG aqueous solution to quickly generate the target magnetic hydrogel. The chitosan–PEG hydrogels could form quickly through dynamic Schiff-base cross-linkage between amine groups of chitosan and benzaldehyde groups on DF-PEG termini. It was noticeable that the hydrogels healed itself automatically without any external stimuli. Figure 20 demonstrated the excellent self-healing capacity. This novel magnetic seal-healing hydrogel might have potential to be used in biological, medical, and environmental fields.

4.2   Self-Healing Hydrogels (Host–Guest)

Cyclodextrins (CDs) are water-soluble cyclic oligomers of D-(+)-glucose units bound to each other through α-1,4-glucose bonding. CDs of 6, 7, and 8 glucose units are called α-, β-, and γ-CDs, respectively. CDs can interact selectively with hydrophobic compounds of a size and shape matching their cavities to form inclusion complexes. Thus, many supramolecular hydrogels based on CDs inclusion complex with guest-containing polymers have been prepared. Self-healing properties of those based on host–guest interactions have been addressed. This work provided a novel supramolecular hydrogels [56] made of copolymers of N,N'-dimethylacrylamide (DMA) modified with cholic acid (CA, the most abundant bile acid in humans and many other species) and β-CD, respectively (Fig. 21). The dynamically reversible host−guest complexation built reasonably good mechanical properties of the cross-linked polymer network. The natural origin of the constituents made the hydrogels suitable candidates for biomedical applications.

Fig. 19 (continued) well as for the drugs (DOX, PTX, and Avastin). Statistical analysis (nD5) was performed with a Log-Rank Mantel–Cox test (PD0.006). Survival cutoff criteria included tumor ulceration or compassionate euthanasia, when the aggregate tumor burden >1 cm in diameter or if tumor impedes eating, urination, defecation, or ambulation. Arrow represents the day of hydrogel implantation (day 22 post tumor induction). (**h**) Heat-map summary of gene expression profiling of the miRs and their related genes that play key roles in cancer progression and migration
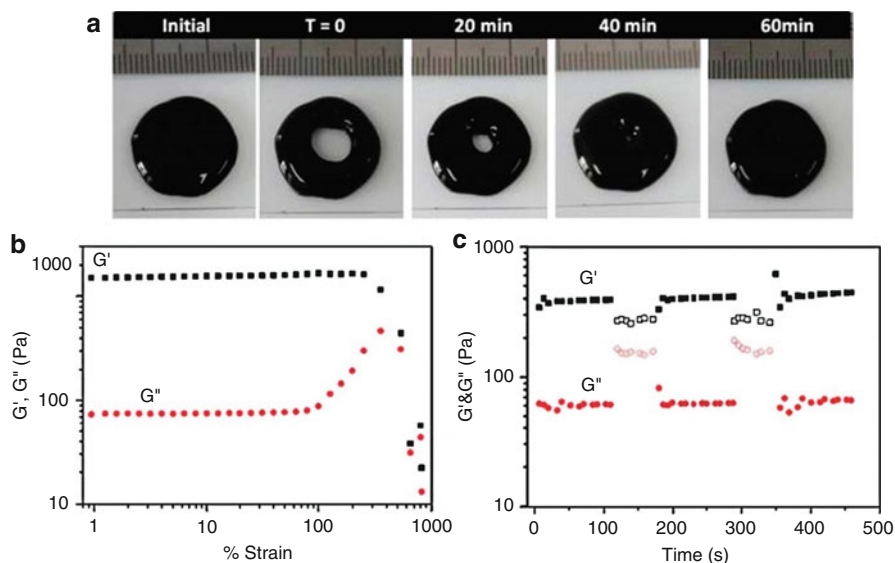
Fig. 20 (**a**) Photos taken during the self-healing process of the hydrogel. (**b**) Rheology analyses of the magnetic self-healing hydrogel. The storage moduli G′ and loss moduli G″ from strain amplitude sweep. (**c**) G′ and G″ from continuous strain sweep with alternate small oscillation force (g = 1% strain, solid dots) and large one (g = 200%, hollow dots)

Cholic acid residue   β-Cyclodextrin residue   Adamantane derivative
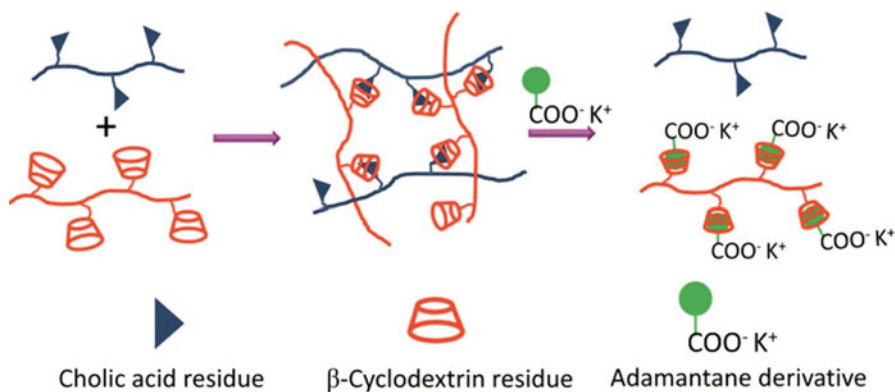
Fig. 21 Illustration of the formation of,P(N,N′-dimethylacrylamide-cholic acid-based methacrylate monomer)/P(N,N′-dimethylacrylamide-p-nitrophenyl acrylate and amino-CD) hydrogel and its dissociation triggered by the addition of potassium 1-adamantylcarboxylate (K-Ada)

4.3   Self-Healing Hydrogels (Hydrogen Bonds)

A series of novel self-healing pH-sensitive biodegradable hydrogels [57] based on cytosine- (C) and guanosine (G)-modified hyaluronic acid (HA) were prepared via hydrogen bonding under physiological conditions, with 1,6-hexamethylenediamine

(HMDA) as a bridging unit between nucleobase and HA. The lowest gel concentration, gelling time, pH-sensitivity, self-healing behavior, rheological properties, morphology, swelling ratio, degradation kinetics, and drug delivery behavior of HA-HMDA-C, HA-HMDA-G, and HA-HMDA-C/G hydrogels were investigated. As shown in Fig. 22, the series of pH-responsive self-healing hydrogels exhibited suitable gelling time, good rheology properties, high swelling ratio, biodegradability, effective drug loading capacity, and sustained drug release ability under physiological conditions. More important, these hydrogels could be attractive candidates for short- and medium-term injectable drug delivery systems, tissue engineering, cell scaffold materials, and regenerative medicine.

4.4   Self-Healing Hydrogels (Hydrophobic–Hydrophilic)

Hydrophobic interactions play a dominant role in the formation of large biological systems. These interactions can be generated in synthetic hydrogels by incorporation of hydrophobic sequences within the hydrophilic polymer network chains. The hydrogels [58] without a chemical cross-linker exhibited unique properties due to the strong hydrophobic interactions. They could only be dissolved in SDS solutions demonstrating the physical nature of cross-links. Results of dynamic light scattering and rheological and mechanical measurements showed that the hydrophobic associations between the blocks of stearyl methacrylate (C18) or dococyl acrylate (C22) units prevented water solubility and flow, while the dynamic nature of the junction zones provided homogeneity and self-healing properties together with a high degree of toughness. When fractured, the hydrogels formed using C18 associations could be repaired by bringing together fractured surfaces to self-heal at room temperature as shown in Fig. 23. The hydrogels without a chemical cross-linker exhibited unique properties. Strong hydrophobic associations between the blocks of C18 or C22 prevented dissolution in water and flow.

5   Conclusion

This chapter delivers a brief overview at functional hydrogels, especially adsorption hydrogels, stimuli-responsive hydrogels, and self-healing hydrogels. Due to the unique structure and properties, hydrogels can be used as adsorption materials for water treatment, drug separation and condition-controlled delivery system, sensors and actuators, and many other smart materials.

6   Future Scope

After decades of investigation, significant accomplishments in the development and characterization of hydrogels have been achieved, and the application of hydrogels has been spread to many aspects, such as green materials, new energy,

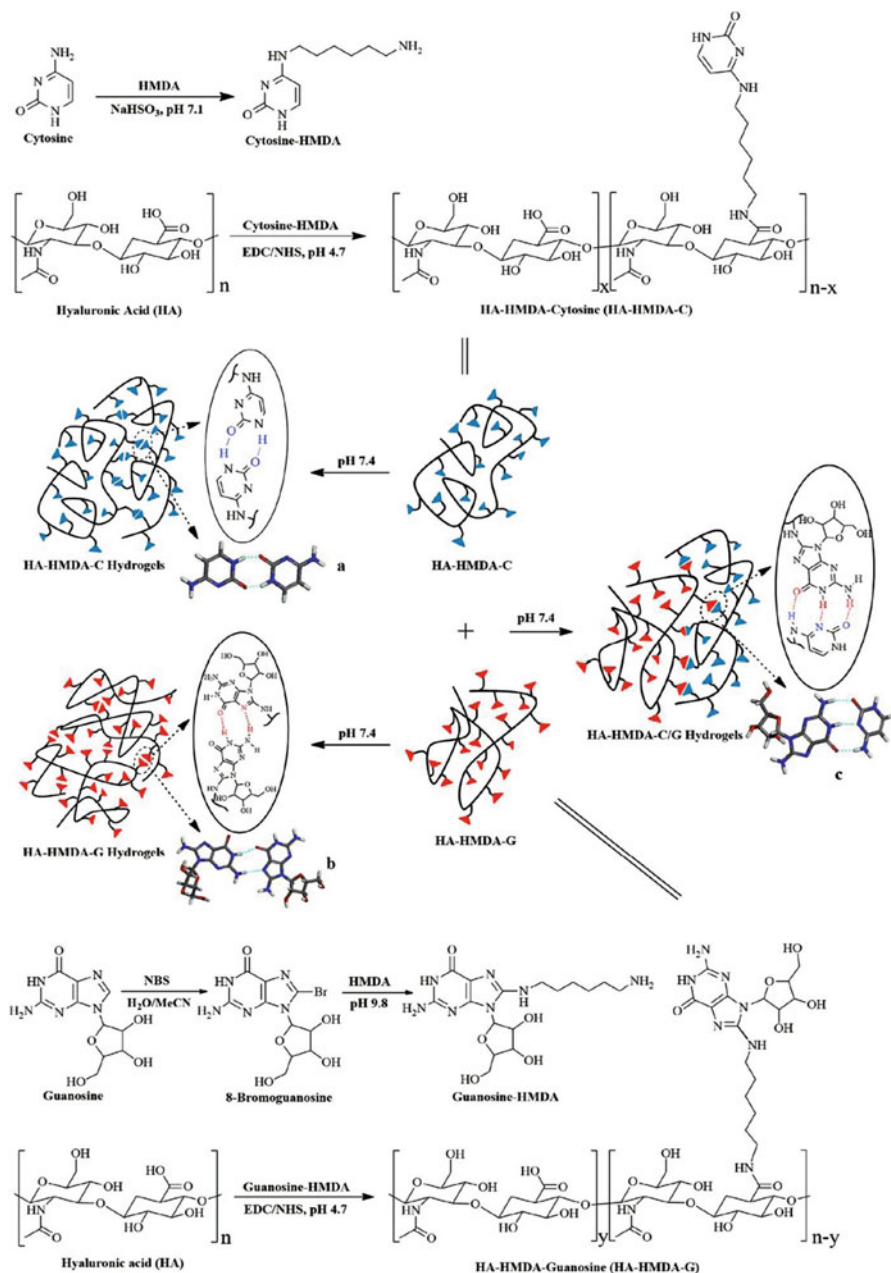**Fig. 22** Schematic illustration of synthesis routes of HA-HMDA-C and HA-HMDA-G and the formation of modified HA hydrogels via hydrogen bonding. The sketches of hydrogen bonds between cytosine and guanosine themselves or each other were carried out by computer simulations using Materials Studio 5.0 (Accelrys, San Diego, USA): (*a*) cytosines, (*b*) guanosines, and (*c*) cytosine and guanosine
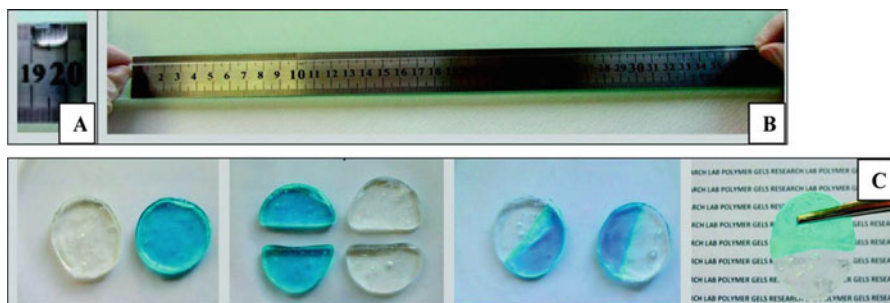
Fig. 23 Photographs before (**a**) and after stretching of a hydrogel sample formed in 0.5 M NaCl (**b**). (**c**) Photographs of two hydrogel samples formed in 0.5 M NaCl. One of the gel samples is colored with methylene blue for clarity. After cutting into two pieces and pressing the fractured surfaces together, they merge into a single piece

biomedicine, etc. The future hydrogels must be more and more smart. The trends of the hydrogel application would be on-demand deformation, artificial organs, wearable devices, etc. Meanwhile, more fundamental researches are necessary to make clear the mechanism of the unique properties of hydrogels.

References

1. Aimetti AA, Machen AJ, Anseth KS (2009) Poly(ethylene glycol) hydrogels formed by thiol-ene photopolymerization for enzyme-responsive protein delivery. Biomaterials 30:6048–6054
2. Bencherif SA, Siegwart DJ, Srinivasan A, Horkay F, Hollinger JO, Washburn NR, Matyjaszewski K (2009) Nanostructured hybrid hydrogels prepared by a combination of atom transfer radical polymerization and free radical polymerization. Biomaterials 30:5270–5278
3. Fekete T, Borsa J, Takács E, Wojnárovits L (2016) Synthesis of cellulose-based superabsorbent hydrogels by high-energy irradiation in the presence of crosslinking agent. Radiat Phys Chem 118:114–119
4. Freudenberg U, Liang Y, Kiick KL, Werner C (2016) Glycosaminoglycan-based biohybrid hydrogels: a sweet and smart choice for multifunctional biomaterials. Adv Mater 28:8861–8891
5. Gong Y, Gao M, Wang D, Möhwald H (2005) Incorporating fluorescent CdTe nanocrystals into a hydrogel via hydrogen bonding: toward fluorescent microspheres with temperature-responsive properties. Chem Mater 17:2648–2653
6. Xing B, Yu C, Chow K, Ho P, Fu D, Xu B (2002) Hydrophobic interaction and hydrogen bonding cooperatively confer a vancomycin hydrogel: a potential candidate for biomaterials. J Am Chem Soc 124:14846–14847
7. Yu LHAY (2013) Directed self-assembly of microscale hydrogels by electrostatic interaction. Biofabrication 5:035004
8. Osman SK, Brandl FP, Zayed GM, Teßmar JK, Göpferich AM (2011) Cyclodextrin based hydrogels: inclusion complex formation and micellization of adamantane and cholesterol grafted polymers. Polymer 52:4806–4812

9. Maity I, Mukherjee TK, Das AK (2014) Photophysical study of a stacked-sheet nanofibril forming peptide Bolaamphiphile hydrogel. New J Chem 38:376–385

10. Buwalda SJ, Amgoune A, Bourissou D (2016) PEG–PLGA copolymers bearing carboxylated side chains: novel hydrogels with enhanced crosslinking via ionic interactions. J Polym Sci A Polym Chem 54:1222–1227

11. Ricciardi R, Auriemma F, Gaillet C, De Rosa C, Lauprêtre F (2004) Investigation of the crystallinity of freeze/thaw poly(vinyl alcohol) hydrogels by different techniques. Macromolecules 37:9510–9516

12. Garcia-Schwarz G, Santiago JG (2012) Integration of on-chip isotachophoresis and functionalized hydrogels for enhanced-sensitivity nucleic acid detection. Anal Chem 84:6366–6369

13. Guillon M, Bilton S, Bleshoy H, Guillon JP, Lydon DPM (1985) Limbal changes associated with hydrogelcontact lens wear. J Br Cont Lens Assoc 8:15–19

14. Murakami K, Aoki H, Nakamura S, Nakamura S, Takikawa M, Hanzawa M, Kishimoto S, Hattori H, Tanaka Y, Kiyosawa T, Sato Y, Ishihara M (2010) Hydrogel blends of chitin/chitosan, fucoidan and alginate as healing-impaired wound dressings. Biomaterials 31:83–90

15. Peng N, Wang Y, Ye Q, Liang L, An Y, Li Q, Chang C (2016) Biocompatible cellulose-based superabsorbent hydrogels with antimicrobial activity. Carbohydr Polym 137:59–64

16. Shahbuddin M, Bullock A, Macneil S, Rimmer S (2014) Glucomannan-poly(N-vinyl Pyrrolidinone) bicomponent hydrogels for wound healing. J Mater Chem B 2(6):727–738

17. Yun J, Jin D, Lee Y, Kim H (2010) Photocatalytic treatment of acidic waste water by electrospun composite nanofibers of pH-sensitive hydrogel and TiO_2. Mater Lett 64(22):2431–2434

18. Xiao M, Hu JC (2017) Cellulose/chitosan composites prepared in ethylene diamine/potassium thiocyanate for adsorption of heavy metal ions. Cellulose 24:2545–2557

19. Wu SP, Dai XZ, Kan JR, Shilong FD, Zhu MY (2017) Fabrication of carboxymethyl chitosan–hemicellulose resin for adsorptive removal of heavy metals from wastewater. Chin Chem Lett 28:625–632

20. Liu Z, Wang HS, Liu C, Jiang YJ, Yu G, Mu XD, Wang XY (2012) Magnetic cellulose-chitosan hydrogels prepared from ionic liquids as reusable adsorbent for removal of heavy metal ions. Chem Commun 48:7350–7352

21. Ayoub A, Venditti RA, Pawlak JJ, Salam A, Hubbe MA (2013) Novel hemicellulose–chitosan biosorbent for water desalination and heavy metal removal. ACS Sustain Chem Eng 1:1102–1109

22. Wei W, Kim S, Song MH, Bediako JK, Yun YS (2015) Carboxymethyl cellulose fiber as a fast binding and biodegradable adsorbent of heavy metals. J Taiwan Inst Chem Eng 57:104–110

23. Ge H, Huang HL, Xu M, Chen Q (2016) Cellulose/poly(ethylene imine) composites as efficient and reusable adsorbents for heavy metal ions. Cellulose 23:2527–2537

24. Zhou YM, Fu SY, Zhang LL, Zhan HY, Mikhail VL (2014) Use of carboxylated cellulose nanofibrils-filled magnetic chitosan hydrogel beads as adsorbents for Pb(II). Carbohydr Polym 101:75–82

25. Luo XB, Guo B, Luo JM, Deng F, Zhang SY, Luo SL, John C (2015) Recovery of lithium from wastewater using development of li ion-imprinted polymers. ACS Sustain Chem Eng 3:460–467

26. Chen PP, Liu XY, Jin RD, Nie WY, Zhou YF (2017) Dye adsorption and photo-induced recycling of hydroxypropyl cellulose/molybdenum disulfide composite hydrogels. Carbohydr Polym 167:36–43

27. Rudzinski WE, Chipuk T, Dave AM, Kumbar SG, Aminabhavi TM (2003) pH-sensitive acrylic-based copolymeric hydrogels for the controlled release of a pesticide and a micronutrient. J Appl Polym Sci 87:394–403

28. Aouada FA, de Moura MA, Orts WJ, Mattoso LHC (2010) Polyacrylamide and methylcellulose hydrogel as delivery vehicle for the controlled release of paraquat pesticide. J Mater Sci 45:4977–4985

29. Abd El-Mohdy HL, Hegazy EA, El-Nesr EM, El-Wahab MA (2012) Removal of some pesticides from aqueous solutions using PVP/(AAc-co-Sty) hydrogels prepared by gamma radiation. J Macromol Sci Part A Pure Appl Chem 49:814–827

30. Chen LY, Tian ZG, Du YM (2004) Synthesis and pH sensitivity of carboxymethyl chitosan-based polyampholyte hydrogels for protein carrier matrices. Biomaterials 25:3725–3732
31. Hennink WE, Talsma H, Borchert JCH, De Smedt SC, Demeester J (1996) Controlled release of proteins from dextran hydrogels. J Control Release 39:47–55
32. Vermonden T, Censi R, Hennink WE (2012) Hydrogels for protein delivery. Chem Rev 112:2853–2888
33. Shao S, Cui EM, Xue HM, Huang HY, Liu GL (2015) Sustained knock down of PPARγ and bFGF presentation in collagen hydrogels promote MSC osteogenesis. Open Life Sci 10(1):479–489
34. Jiang YJ, Chen J, Deng C, Suuronen EJ, Zhong Z (2014) Click hydrogels, microgels and nanogels: emerging platforms for drug delivery and tissue engineering. Biomaterials 35:4969–4985
35. Qiu Y, Park K (2012) Environment-sensitive hydrogels for drug delivery. Adv Drug Deliv Rev 64:49–60
36. Bhattarai N, Gunn J, Zhang MQ (2010) Chitosan-based hydrogels for controlled, localized drug delivery. Adv Drug Deliv Rev 62:83–99
37. Abureesh MA, Oladipo AA, Gazi M (2016) Facile synthesis of glucose-sensitive chitosan–poly(vinyl alcohol) hydrogel: drug release optimization and swelling properties. Int J Biol Macromol 90:75–80
38. Zhang XZ, Wu DQ, Chu CC (2004) Synthesis, characterization and controlled drug release of thermosensitive IPN–PNIPAAm hydrogels. Biomaterials 25:3793–3805
39. Zhao CW, Zhuang XL, He P, Xiao CS, He CL, Sun JR, Chen XS, Jing XB (2009) Synthesis of biodegradable thermo- and pH-responsive hydrogels for controlled drug release. Polymer 50:4308–4316
40. Huang HL, Wang XH, Ge H, Xu M (2016) Multifunctional magnetic cellulose surface-imprinted microspheres for highly selective adsorption of artesunate. ACS Sustain Chem Eng 4:3334–3343
41. Manal F, Abou T, Abdel-Aal SE, El-Kelesh NA, Hegazy ESA (2007) Adsorption and controlled release of chlortetracycline HCl by using multifunctional polymeric hydrogels. Eur Polym J 43:468–477
42. Lee YJ, Braun PV (2003) Tunable inverse opal hydrogel pH sensors. Adv Mater 15:563–566
43. Richter A, Paschew G, Klatt S, Lienig J, Arndt K, Adler PH (2008) Review on hydrogel-based pH sensors and microsensors. Sensors-Basel 8(1):561–581
44. Killer M, Keeley EM, Cruise GM, Schmitt A, McCoy MR (2011) MR imaging of hydrogel filament embolic devices loaded with superparamagnetic Iron oxide or gadolinium. Neuroradiology 53(6):449–456
45. Soto AM, Koivisto JT, Parraga JE, Silva-Correia J, Oliveira JM, Reis RL, Kellomäki M, Hyttinen J, Figueiras E (2016) Optical projection tomography technique for image texture and mass transport studies in hydrogels based on Gellan gum. Langmuir 32(20):5173–5182
46. Takehara H, Nagaoka A, Noguchi J, Akagi T, Kasai H, Ichiki T (2016) Implantable microfluidic device with hydrogel permeable membrane for delivering chemical compounds and imaging neural cells in living mice. J Photopolym Sci Technol 29(4):513–518
47. Emileh A, Vasheghani-Farahani E, Imani M (2007) Swelling behavior, mechanical properties and network parameters of pH- and temperature-sensitive hydrogels of poly((2-dimethyl amino) ethyl methacrylate-co-butyl methacrylate). Eur Polym J 43(5):1986–1995
48. Luo RC, Cao Y, Shi P, Chen CH (2014) Near-infrared light responsive multi-compartmental hydrogel particles synthesized through droplets assembly induced by superhydrophobic surface. Small 10(23):4886–4894
49. Chen J, Sheng KX, Luo PH, Li C, Shi GQ (2012) Graphene hydrogels deposited in nickel foams for high-rate electrochemical capacitors. Adv Mater 24:4569–4573
50. Kim SJ, Lee CK, Lee YM, Kim IY, Kim SI (2003) Electrical/pH-sensitive swelling behavior of polyelectrolyte hydrogels prepared with hyaluronic acid–poly(vinyl alcohol) interpenetrating polymer networks. React Funct Polym 55(3):291–298

51. Konieczynska MD, Grinstaff MW (2017) On-demand dissolution of chemically cross-linked hydrogels. Acc Chem Res 50:151–160
52. Le XX, Lu W, Xiao H, Wang L, Ma CX, Zhang JW, Huang YJ, Chen T (2017) Fe^{3+}-, pH-, thermoresponsive supramolecular hydrogel with multishape memory effect. ACS Appl Mater Interfaces 9:9038–9044
53. Xing YZ, Cheng EJ, Yang Y, Chen P, Zhang T, Sun YW, Yang ZQ, Liu DS (2011) Self-assembled DNA hydrogels with designable thermal and enzymatic responsiveness. Adv Mater 23:1117–1121
54. João C, Nuria O, Mariana A, Song HS, Natalie A (2016) Self-assembled RNA-triple-helix hydrogel scafold for microRNA modulation in the tumour microenvironment. Nat Mater 15:353–363
55. Zhang YL, Yang B, Zhang XY, Xu LX, Tao L, Li SX, Wei Y (2012) A magnetic self-healing hydrogel. Chem Commun 48:9305–9307
56. Jia YG, Zhu XX (2015) Self-healing supramolecular hydrogel made of polymers bearing cholic acid and β-cyclodextrin pendants. Chem Mater 27:387–393
57. Ye X, Li X, Shen YQ, Chang GJ, Yang JX, Gu ZW (2017) Self-healing pH-sensitive cytosine- and guanosine-modified hyaluronic acid hydrogels via hydrogen bonding. Polymer 108:348–360
58. Deniz CT, Murat S, Wilhelm O, Oguz O (2011) Tough and self-healing hydrogels formed via hydrophobic interactions. Macromolecules 44:4997–5005